

Deformation Dependence of Breathing Oscillations in Bose - Fermi Mixtures at Zero Temperature

Tomoyuki Maruyama,^{1,2,3} Tike's Yamamoto,⁴ Takushi Nishimura,⁵ and Hiroyuki Yabu⁴

¹*College of Bioresource Sciences, Nihon University, Fujisawa 252-0880, Japan*

²*Advanced Science Research Center, Japan Atomic Energy Agency, Tokai 319-1195, Japan*

³*National Astronomical Observatory of Japan,*

2-21-1 Osawa, Mitaka, Tokyo 181-8588, Japan

⁴*Department of Physics, Ritsumeikan University, Kusatsu 525-8577, Japan*

⁵*Department of Physics, Tokyo Metropolitan University, Hachioji, Tokyo 192-0397, Japan*

(Dated: February 21, 2022)

We study the breathing oscillations in bose-fermi mixtures in the axially-symmetric deformed trap of prolate, spherical and oblate shapes, and clarify the deformation dependence of the frequencies and the characteristics of collective oscillations. The collective oscillations of the mixtures in deformed traps are calculated in the scaling method. In largely-deformed prolate and oblate limits and spherical limit, we obtain the analytical expressions of the collective frequencies. The full calculation shows that the collective oscillations become consistent with the analytically-obtained frequencies when the system is deformed into both prolate and oblate regions. The complicated changes of oscillation characters are shown to occur in the transcendental regions around the spherically-deformed region. We find that these critical changes of oscillation characters are explained by the level crossing behaviors of the intrinsic oscillation modes. The approximate expressions are obtained for the level crossing points that determine the transcendental regions. We also compare the results of the scaling methods with those of the dynamical approach.

PACS numbers: 03.75.Kk,67.10.Jn,51.10.+y

I. INTRODUCTION

Study of the ultracold atomic gases have been made many progresses in many-body quantum theory through the Bose-Einstein condensates (BEC) [1–4], two boson mixtures [5, 6], degenerate atomic Fermi gases [7], and Bose-Fermi (BF) mixing gases [5, 8–10]. In particular, the BF mixtures, a typical example in which particles obeying different quantum statistics are intermingled, attract physical interest to obtain new knowledge of many-body quantum systems because of a large variety of combinations of atomic species and controllability of the atomic interactions using the Feshbach resonance [11].

A variety of theoretical studies have been done on the BF mixtures: static properties [12–17], phase diagrams and phase separation phenomena [18–21], instability [22–24] and collective excitations [17, 25–34].

The researches on the trapped atomic gases of the Yb isotopes have been performed by Kyoto university group: the BEC [35] and the Fermi-degeneracy [36]. They also succeeded in realizing the BF mixtures of the isotopes. The Yb consists of many kinds of isotopes— five bosons ($^{168,170,172,174,176}\text{Yb}$) and two fermions ($^{171,173}\text{Yb}$), which give a variety of combinations in the BF mixtures. The scattering lengths of the boson-fermion interactions have been determined experimentally by the group [36–40], and the experimental studies of the ground state properties and the collective oscillations of the BF mixtures is now under progressing.

In many characteristic properties, the spectrum of the collective excitations is an important diagnostic signal of these systems; they commonly appear in many-particle systems and are often sensitive to the inter-particle interaction and the structure of the ground and excited states. Using a dynamical approach to solve time-developments of the oscillation states with the time-dependent Gross-Pitaevskii (TDGP) and Vlasov equations, we have studied the monopole [30, 31], dipole [32] and quadrupole [33] oscillations of the BF mixtures in the spherical traps and the breathing oscillations in the largely prolate deformed system [34]. In these works, we found that the oscillational motions of the BF mixtures include various modes, and that, though the intrinsic frequencies are somewhat different from those in the sum-rule [17, 27], the dynamical calculations give consistent results with the random phase approximation (RPA) [25, 26] in the early stage of time development.

The oscillations are decoupled into the longitudinal and transverse oscillation modes in the largely prolate deformed system, and into the monopole and quadrupole oscillation modes in the completely spherical system. However, the mixing behavior of these modes is not known in the deformed region between the above two extreme conditions.

We studied the deformation dependence of breathing oscillations in the two-component fermi gases using the scaling approach[41], and found that the breathing oscillations can be described as superpositions of the four oscillation modes: the longitudinal and transverse oscillations with in-phase and out-of-phase[42]. In the aspect of the mixing of these modes, the characteristic mixing behaviors for the breathing oscillations are found in the oblate, spherical and prolate traps, respectively.

In BF mixtures, it should be noted that the in-phase and out-of-phase oscillations are not intrinsic modes in oscillations because the two components obey different statistics. Thus, the BF mixtures are expected to show different behaviors in the mode mixing and resonances at the level crossing points from the two-component fermi gases.

In this work, then, we investigate the deformation dependence in the breathing oscillations of the BF mixtures by examining mixing properties of the longitudinal and transverse oscillations. For this purpose we use the scaling approach, which is an approximation of the RPA [43–45], and describe collective

oscillations with macroscopic picture. This method have reproduced the intrinsic frequencies of the BF breathing oscillations calculated in the time-dependent simulation [34], and can clearly demonstrate the mixing properties,

Though this scaling method is thought to describe the collective oscillations within the linear response regime, the nonlinear calculation was applied to the oscillations of BEC [46], which reproduced the experimental results by Ref. [47] very well. Also, the method was used in the study of the oscillations of non-condensed bose gases [48] and the quasi-low dimension gases [49]. In the next section, we give a brief explanation of the scaling method and discuss the mixing of the boson and fermion oscillations in extreme conditions. In Sec. III, we show the results in various deformed traps in the scaling method. In Sec. IV, we compare the collective oscillation modes obtained in the scaling method with those in the dynamical approach based on the TDGP+Vlasov equation. The summary of the present work is given in Sec. V.

II. COLLECTIVE OSCILLATIONS IN THE SCALING METHOD

Let's consider the oscillation behaviors of the mixture in the deformed system, and take up the collective modes from the macroscopic point of view.

In order to calculate the oscillation modes, we use the scaling method, for which we only give a brief explanation, so that, for the details, the readers should consult the previous paper. [34]. Based on the method, we also discuss the mixing behaviors of the boson and fermion oscillations, which has not been done in detail before.

A. Total Energy of BF mixtures and Scaled Variables

Let's consider the zero-temperature BF mixture of dilute boson and one-component-fermion gases trapped in an axially symmetric potential of the symmetry z -axis; the interatomic interactions are assumed to be zero-range with no fermion-fermion interactions. In the Hartree-Fock approximation, the total energy is represented by a functional of the condensed boson wave function ϕ_c , and the n -th fermion single-particle wave functions ψ_n :

$$\begin{aligned}
 E_T = \int d^3r \left[\frac{\hbar^2}{2M_B} N_b \nabla_r \phi_c^\dagger(\mathbf{r}) \nabla_r \phi_c(\mathbf{r}) + \frac{M_B}{2} (\Omega_T^2 r_T^2 + \Omega_L^2 z^2) N_b \phi_c^\dagger(\mathbf{r}) \phi_c(\mathbf{r}) + \frac{2\pi\hbar^2 a_{BB}}{M_{Bu}} \{N_b \phi_c^\dagger(\mathbf{r}) \phi_c(\mathbf{r})\}^2 \right. \\
 + \frac{\hbar^2}{2M_f} \sum_{n=1}^{N_f} \nabla_r \psi_n^\dagger(\mathbf{r}) \nabla_r \psi_n(\mathbf{r}) + \frac{1}{2} M_F \omega_f^2 (\Omega_T^2 r_T^2 + \Omega_L^2 z^2) \sum_{n=1}^{N_f} \psi_n^\dagger(\mathbf{r}) \psi_n(\mathbf{r}) \\
 \left. + 2\pi\hbar^2 \frac{M_B + M_F}{M_B M_F} a_{BF} N_b \phi_c^\dagger(\mathbf{r}) \phi_c(\mathbf{r}) \sum_{n=1}^{N_f} \psi_n^\dagger(\mathbf{r}) \psi_n(\mathbf{r}) \right], \quad (1)
 \end{aligned}$$

where $M_{B,F}$ are the boson and fermion masses, $a_{BB,BF}$ are the s-wave scattering lengths of the boson-boson and boson-fermion interactions, and $N_{b,f}$ are the number of bosons and fermions. We assume the trapping potentials of the similar harmonic shape with the transverse and longitudinal trapping frequencies (Ω_T, Ω_L) for bosons and $(\omega_f \Omega_T, \omega_f \Omega_L)$ for fermions. For future convenience, we define the frequency parameters: $\Omega_B \equiv (\Omega_T^2 \Omega_L)^{1/3}$, $\omega_T = \Omega_T / \Omega_B$, and $\omega_L = \Omega_L / \Omega_B = \omega_T^{-1/2}$.

Here, we use the time coordinate τ scaled with Ω_B^{-1} . The scaled wave functions $\phi_\lambda(\mathbf{r}, t)$ and $\psi_{\lambda,n}(\mathbf{r}, \tau)$ for bosons and fermions are introduced from the ground-state one-body wave functions, $\phi_c^{(g)}$ and $\psi_n^{(g)}$:

$$\phi_\lambda(\mathbf{r}, t) = e^{iM_B \xi_B(\mathbf{r}, t)/\hbar} e^{\lambda_{BT}(t) + \frac{1}{2} \lambda_{BL}(t)} \phi_c^{(g)}(e^{\lambda_{BT}(t)} \mathbf{r}_T; e^{\lambda_{BL}(t)} z), \quad (2)$$

$$\psi_{\lambda,n}(\mathbf{r}, \tau) = e^{iM_F \xi_F(\mathbf{r}, t)/\hbar} e^{\lambda_{FT}(t) + \frac{1}{2} \lambda_{FL}(t)} \psi_n^{(g)}(e^{\lambda_{FT}(t)} \mathbf{r}_T; e^{\lambda_{FL}(t)} z) \quad (3)$$

with

$$\xi_a(\mathbf{r}, \tau) = \frac{1}{2} \left\{ \dot{\lambda}_{Ta}(\tau) r_T^2 + \dot{\lambda}_{La}(\tau) z^2 \right\}, \quad (a = B, F) \quad (4)$$

where the collective coordinates, $\lambda_{BT}, \lambda_{BL}, \lambda_{FT}, \lambda_{FL}$, boson transverse breathing (BTB), describes the boson longitudinal breathing (BLB), fermion transverse breathing (FTB) and fermion longitudinal breathing (FLB) oscillation modes respectively, and $\dot{\lambda}$'s are the time-derivatives. It turns out later that these four modes are completely decoupled in the BF mixtures of no interactions: $a_{BB} = a_{BF} = 0$.

Using the wave-functions (2) and (3) for the total energy functional (1), we obtain,

$$\begin{aligned}
E_T = & \frac{M_B}{2\hbar^2} \int d^3r (\nabla_r \xi_B)^2 \rho_B + \frac{1}{2} e^{2\lambda_{BT}} (T_{B,1} + T_{B,2}) + \frac{1}{2} e^{2\lambda_{BL}} T_{B,3} \\
& + \frac{M_B}{2} \Omega_B^2 \int d^3r \left\{ \omega_T^2 e^{-2\lambda_{BT}} (r_1^2 + r_2^2) + \omega_L^2 e^{-2\lambda_{BL}} z^2 \right\} \rho_B(\mathbf{r}) \\
& + \frac{2\pi\hbar^2 a_{BB}}{M_{BB}} e^{2\lambda_{BT} + \lambda_{BL}} \int d^3r \rho_B^2(\mathbf{r}), \\
& + \frac{M_F}{2\hbar^2} \int d^3r (\nabla_r \xi_F)^2 \rho_F + \frac{1}{2} e^{2\lambda_{FT}} (T_{F,1} + T_{F,2}) + \frac{1}{2} e^{2\lambda_{FL}} T_{F,3} \\
& + \frac{M_F}{2} \omega_f^2 \Omega_F^2 \int d^3r \left\{ \omega_T^2 e^{-2\lambda_{FT}} (r_1^2 + r_2^2) + \omega_L^2 e^{-2\lambda_{FL}} z^2 \right\} \rho_F(\mathbf{r}), \\
& + 2\pi\hbar^2 \frac{M_B + M_F}{M_B M_F} a_{BF} e^{2\lambda_{BT} + \lambda_{BL} + 2\lambda_{FT} + \lambda_{FL}} \int d^3r \rho_B(e^{\lambda_{BT}} \mathbf{r}_T; e^{\lambda_{BL}} z) \rho_F(e^{\lambda_{FT}} \mathbf{r}_T; e^{\lambda_{FL}} z), \quad (5)
\end{aligned}$$

where

$$\begin{aligned}
T_{B,i} &= \frac{\hbar^2}{M_B} \int d^3r \left| \frac{\partial}{\partial r_i} \phi(\mathbf{r}) \right|^2, \quad (i = 1, 2, 3) \\
T_{F,i} &= \frac{\hbar^2}{M_F} \sum_n \int d^3r \left| \frac{\partial}{\partial r_i} \psi_n(\mathbf{r}) \right|^2, \quad (i = 1, 2, 3) \\
\rho_B(\mathbf{r}) &= N_b |\phi_c(\mathbf{r})|^2, \quad \rho_F(\mathbf{r}) = \sum_{n=1}^{N_f} |\psi_n(\mathbf{r})|^2.
\end{aligned}$$

In order to obtain the ground state of the system, we use the Thomas-Fermi (TF) approximation:

$$T_B(\mathbf{r}) = 0, \quad T_{F,1}(\mathbf{r}) = T_{F,2}(\mathbf{r}) = T_{F,3}(\mathbf{r}) = \frac{1}{5} (6\pi^2)^{\frac{2}{3}} \hbar^2 \rho_F(\mathbf{r})^{\frac{5}{3}}. \quad (6)$$

In order to simplify the analytic calculation, we introduce the dimensionless constants and variables:

$$\begin{aligned}
h &= \omega_f \frac{M_B(M_B + M_F)}{M_F^2} \frac{a_{BF}}{a_{BB}}, \quad \mathbf{x} = \frac{4}{3\pi} \frac{M_F^4 \Omega_F^5 a_{BB}}{\hbar M_B^3 \Omega_B^4} (\omega_T r_1, \omega_T r_2, \omega_L z), \\
n_B &= \frac{128}{9\pi} \left(\frac{M_F}{M_B} \right)^8 \omega_f^{10} a_{BB}^3 \rho_B, \quad n_F = \frac{32}{9\pi} \frac{M_F^9 (M_B + M_F)^3}{M_B^{12}} \omega_f^{12} a_{BB}^3 \rho_F, \quad (7)
\end{aligned}$$

and the scaled dimensionless total energy of the ground state is written by

$$\begin{aligned}
\tilde{E}_T^{(0)} &= \frac{4^9}{3^7 \pi^6 \hbar^4} \frac{M_F^{28} \Omega_F^{35}}{M_B^{24} \Omega_B^{30}} a_{BB}^8 E_T(\boldsymbol{\lambda} = 0, \dot{\boldsymbol{\lambda}} = 0) \\
&= \int d^3x \left\{ x^2 n_B + \frac{1}{2} n_B^2 + \frac{3}{5} n_F^{\frac{5}{3}} + x^2 n_F + h n_B n_F \right\}, \quad (8)
\end{aligned}$$

where $x^2 = |\mathbf{x}|^2$.

The TF equations become

$$n_B + hn_F = e_B - x^2, \quad n_F^{\frac{2}{3}} + hn_B = e_F - x^2, \quad (9)$$

where e_B and e_F are the scaled boson and fermion chemical potentials.

B. Collective Oscillations in Scaling Method

We introducing the vector notation for the oscillation amplitudes:

$$\boldsymbol{\lambda} = \begin{pmatrix} \lambda_B \\ \lambda_F \end{pmatrix}, \quad \lambda_B = \begin{pmatrix} \lambda_{BT} \\ \lambda_{BL} \end{pmatrix}, \quad \lambda_F = \begin{pmatrix} \lambda_{FT} \\ \lambda_{FL} \end{pmatrix}, \quad (10)$$

where two-component matrices λ_B and λ_F are the bosonic and fermionic amplitudes. Expanding the total energy (5) to the order of $O(\lambda^2)$, we obtain the oscillation energy in the harmonic approximation:

$$\Delta \tilde{E}_T \equiv \tilde{E}_T - \tilde{E}_T^{(0)} \approx \frac{1}{2} \dot{\boldsymbol{\lambda}} B \dot{\boldsymbol{\lambda}} + \frac{1}{2} \boldsymbol{\lambda} C \boldsymbol{\lambda}. \quad (11)$$

where B and C are 4×4 matrices defined as follows; The matrices B is

$$B = \frac{2}{3} \begin{pmatrix} X_B \tilde{B} & 0 \\ 0 & \frac{1}{\omega_F^2} X_F \tilde{B} \end{pmatrix}, \quad (12)$$

where \tilde{B} is a diagonal matrix: $\tilde{B} = \text{diag}(2/\omega_T^2, 1/\omega_L^2)$ with $\omega_k \equiv \Omega_k/\Omega_B$ ($k = T, L$). And the matrix C as

$$C = \frac{2}{3} \begin{pmatrix} X_B \left(1 - \frac{V_1}{10X_B}\right) \tilde{C}_B & V_1 \tilde{C}_B \\ V_1 \tilde{C}_B & X_F \tilde{C}_F \end{pmatrix}. \quad (13)$$

The 2×2 submatrices \tilde{C}_B and \tilde{C}_F are

$$\tilde{C}_B = \begin{pmatrix} 8 & 2 \\ 2 & 3 \end{pmatrix}, \quad \tilde{C}_F = \begin{pmatrix} 8 - \frac{4V_1}{5X_F} & -\frac{V_1}{5X_F} - \frac{V_2}{X_F} \\ -\frac{V_1}{5X_F} - \frac{V_2}{X_F} & 4 - \frac{3V_1}{10X_F} + \frac{V_2}{2X_F} \end{pmatrix}. \quad (14)$$

with

$$X_{B,F} = \int d^3x x^2 n_{B,F}(\mathbf{x}), \quad (15)$$

$$V_1 = h \int d^3x x^2 \frac{\partial n_B}{\partial x} \frac{\partial n_F}{\partial x}, \quad (16)$$

$$V_2 = h \int d^3x x n_F \frac{\partial n_B}{\partial x}. \quad (17)$$

where $x^2 = |\mathbf{x}|^2$.

From Eq. (11), the oscillation frequency ω and the corresponding amplitude $\boldsymbol{\lambda}$ are determined from the characteristic equation:

$$(B\omega^2 - C) \boldsymbol{\lambda} = 0. \quad (18)$$

The above equation has four kinds of eigenvectors λ_i and the corresponding eigen-frequencies ω_i , which satisfies the orthogonal relation, ${}^t\lambda_i B \lambda_j \propto \delta_{ij}$.

For later convenience, we introduce some intrinsic oscillation frequencies defined from the diagonal components of the matrices B and C :

$$\omega_i = \sqrt{\frac{C_{ii}}{B_{ii}}}, \quad i = 1, 2, 3, 4. \quad (19)$$

which correspond to the boson-transverse (BT), the boson-longitudinal (BL), the fermion-transverse (FT), and the fermion-longitudinal (FL) modes. It should be noted that these modes become eigenvalues of the characteristic equation (18) if the non-diagonal matrix elements are neglected (as it were, diabatic modes). with $i = \text{BT}$ (boson-transverse mode), BL (boson-longitudinal mode). In substitution of the diagonal elements in Eqs. (12) and (13) into Eq. (19), simple calculation gives

$$\begin{aligned} \omega_{BT}^2 &= 4\omega_T^2 \left(1 - \frac{v_B}{10}\right), & \omega_{BL}^2 &= 3\omega_L^2 \left(1 - \frac{v_B}{10}\right), \\ \omega_{FT}^2 &= 4\omega_T^2 \omega_f^2 \left(1 - \frac{v_f}{10}\right), & \omega_{FL}^2 &= \omega_L^2 \omega_f^2 \left(4 - \frac{3v_f}{10} + \frac{v_2}{2}\right) \end{aligned} \quad (20)$$

with $v_B = V_1/X_B$, $v_F = V_1/X_F$, $v_2 = V_2/X_B$, and the corresponding amplitudes are

$$\lambda_{BT} = \begin{pmatrix} \mathbf{u}_T \\ 0 \end{pmatrix}, \quad \lambda_{BL} = \begin{pmatrix} \mathbf{u}_L \\ 0 \end{pmatrix}, \quad \lambda_{FT} = \begin{pmatrix} 0 \\ \mathbf{u}_T \end{pmatrix}, \quad \lambda_{FL} = \begin{pmatrix} 0 \\ \mathbf{u}_L \end{pmatrix},$$

where $\mathbf{u}_T = {}^t(1, 0)$ and $\mathbf{u}_L = {}^t(0, 1)$.

The other intrinsic modes are the bosonic and fermionic modes obtained by diagonalizing the bosonic and fermionic parts of the characteristic equation (18) [34]:

$$[\tilde{B}\omega^2 - (1 - v_B/10)\tilde{C}_B]\lambda_B = 0, \quad [\tilde{B}\omega^2 - \omega_f^2\tilde{C}_F]\lambda_F = 0, \quad (21)$$

which are the oscillations for the frozen boson or fermion distributions.

In the following subsections we consider these modes in three extreme cases, spherical, largely prolate, and oblate deformed traps, and clarify the aspect of the boson and fermion oscillation mixings, which was not clearly given in Ref. [34].

C. Collective Modes in Spherical Trap

First we consider the collective modes of the BF mixture in the spherical trap where $\omega_T = \omega_L = 1$. To simplify the discussion, we take the same trap frequencies of the boson and fermion, $\omega_f = 1$. In this case, the oscillations are decoupled into the monopole and quadrupole modes, where $\lambda_{B,F} \propto \mathbf{u}_M \propto {}^t(1, 1)$ and $\lambda_{B,F} \propto \mathbf{u}_Q \propto {}^t(1, -2)$, respectively.

The monopole oscillation has two modes:

$$\omega_M^2(\pm 1) = \frac{1}{2} \left(9 - \frac{v_B}{2} - \frac{v_F}{2} - \frac{v_2}{2} \pm \sqrt{D_M} \right),$$

$$D_M = \left(1 - \frac{v_B}{2} + \frac{v_F}{2} + \frac{v_2}{2} \right)^2 + v_B v_F.$$

The amplitudes corresponding to $\omega(\pm 1)$ are

$$\lambda_M(+1) = \begin{bmatrix} \left(1 - \frac{v_B}{2} + \frac{v_F}{2} + \frac{v_2}{2} + \sqrt{D_M} \right) \mathbf{u}_M \\ v_F \mathbf{u}_M \end{bmatrix},$$

$$\lambda_M(-1) = \begin{bmatrix} -v_B \mathbf{u}_M \\ \left(1 - \frac{v_B}{2} + \frac{v_F}{2} + \frac{v_2}{2} + \sqrt{D_M} \right) \mathbf{u}_M \end{bmatrix}.$$

The quadrupole oscillation has also two modes:

$$\omega_Q^2(\pm 1) = \frac{1}{2} \left(2 - \frac{v_F}{5} - \frac{v_B}{5} + v_2 \pm \sqrt{D_Q} \right),$$

$$D_Q = \left(2 + v_2 - \frac{v_F}{5} + \frac{v_B}{5} \right)^2 + \frac{4}{25} v_B v_F,$$

and the corresponding amplitudes are

$$\lambda_Q(+1) = \begin{bmatrix} \frac{v_B}{5} \mathbf{u}_Q \\ \left(1 + \frac{v_B}{10} - \frac{v_F}{10} + \frac{v_2}{2} + \frac{1}{2} \sqrt{D_Q} \right) \mathbf{u}_Q \end{bmatrix},$$

$$\lambda_Q(-1) = \begin{bmatrix} \left(1 + \frac{v_B}{10} - \frac{v_F}{10} + \frac{v_2}{2} + \frac{1}{2} \sqrt{D_Q} \right) \mathbf{u}_Q \\ -\frac{v_F}{5} \mathbf{u}_Q \end{bmatrix}.$$

Because of $\partial n_F / \partial x < 0$ when $h < 1$ and $\partial n_F / \partial x > 0$ when $h > 1$ in the boson-populated region, the signs of v_B and v_F become $v_{B,F} < 0$ when $h < 0$ or $h > 1$, and $v_{B,F} > 0$ when $0 < h < 1$.

When $h < 0$ or $h > 1$, then, the $\lambda_M(-1)$ and $\lambda_Q(-1)$ are boson-fermion in-phase, and $\lambda_M(+1)$ and $\lambda_Q(+1)$ are out-of-phase, while the relative phase is opposite when $0 < h < 1$. Thus, in the case of the spherical trap, we find four collective oscillations: the in-phase monopole (IM), the out-of-phase monopole (OM), the in-phase quadrupole (IQ), and the out-of-phase quadrupole (OQ) modes.

In the case of small BF coupling ($0 < h \ll 1$), the boson and fermion oscillation modes almost decouple.

In actual experiments and theoretical calculation discussed later, the boson number is set to be much larger than the fermion number ($N_b \gg N_f$). In the boson-dominant approximation, we can put $|v_B| \ll |v_F|$ because the integral $X_{B,F}$ satisfy the relation $X_B \gg X_F$, and the amplitudes becomes $\lambda_M(+1) \propto {}^t(0, \mathbf{u}_M)$ and $\lambda_Q(+1) \propto {}^t(0, \mathbf{u}_Q)$ approximately. So, in the boson-dominant approximation, the OM and IQ modes become similar with the fermion monopole (FM) and fermion quadrupole (FQ) oscillations.

When $-1 \ll h < 0$, the same argument is available though the relative phase between the boson and fermion oscillations is opposite.

D. Collective Modes in Largely Prolate Deformed Traps

We discuss the collective oscillation modes in largely deformed traps ($\omega_T \gg \omega_L$) when $\omega_f = 1$.

Before discussing the collective oscillation in the full-calculation, we show the bosonic and fermionic intrinsic modes obtained by solving (21).

The boson oscillation has two kinds of oscillation: the boson transverse breathing (BTB) and the boson axial breathing (BAB) modes. The frequencies are

$$\omega_{BTB}^2 \approx 4 \left(1 - \frac{\nu_B}{10}\right) \omega_T^2, \quad \omega_{BAB}^2 \approx \frac{5}{2} \left(1 - \frac{\nu_B}{10}\right) \omega_L^2, \quad (22)$$

and the corresponding amplitudes are $\lambda_B \approx \mathbf{u}_T$ and $\lambda_B \approx \mathbf{u}_{BA} \equiv {}^t(-1/4, 1)$ [34].

The fermionic oscillation also has two modes: the fermion transverse breathing (FTB) and the fermion axial breathing (FAB) modes. The frequencies are

$$\omega_{FTB}^2 \approx 4 \left(1 - \frac{\nu_F}{10}\right) \omega_T^2, \quad \omega_{FAB}^2 \approx \left(4 + \frac{15\nu_2 - 12\nu_F - 4\nu_2\nu_F + \nu_F^2}{40 - 4\nu_F}\right) \omega_L^2, \quad (23)$$

and the corresponding amplitudes are

$$\lambda_F \approx \mathbf{u}_T, \quad \lambda_F \approx \mathbf{u}_{FA} \equiv \begin{pmatrix} -\frac{\nu_2 + \nu_F/5}{4 - 2\nu_F/5} \\ 1 \end{pmatrix}.$$

Now we turn to the collective oscillations obtained by solving (18). In the full calculation, we find that the transverse and axial oscillation modes do not mix in the limit of $\omega_L/\omega_T \rightarrow 0$, so that the mode-mixing of the BTB and FTB, and the BAB and FAB occurs,

The resultant transverse oscillations are the in-phase and out-of-phase transverse breathing (ITB and OTB) modes, the frequencies and the amplitudes of which are

$$\omega_{ITB}^2 \approx 4\omega_T^2, \quad \omega_{OTB}^2 \approx \left[4 - \frac{2}{5}(\nu_B + \nu_F)\right] \omega_T^2,$$

and

$$\lambda_{ITB} \approx \begin{pmatrix} \mathbf{u}_T \\ \mathbf{u}_T \end{pmatrix}, \quad \lambda_{OTB} \approx \begin{pmatrix} -\frac{X_B}{X_F} \mathbf{u}_T \\ \mathbf{u}_T \end{pmatrix} \approx \begin{pmatrix} 0 \\ \mathbf{u}_T \end{pmatrix}.$$

The ITB mode has the same amplitudes of the boson and fermion oscillations, while the OTB mode is very similar to the FTB mode in the boson-dominant approximation ($X_B \ll X_F$).

The axial breathing (AB) oscillations have also two modes; their frequencies are

$$\frac{\omega^2(s)}{\omega_L^2} = \frac{13}{4} - \frac{\nu_B}{8} + \frac{15\nu_2 - 12\nu_F - 4\nu_2\nu_F + \nu_F^2}{80(1 - \frac{\nu_F}{10})} + \frac{s}{2}\sqrt{D_A},$$

$$D_A = \left\{ \frac{3}{2} + \frac{\nu_B}{4} + \frac{15\nu_2 - 12\nu_F - 4\nu_2\nu_F + \nu_F^2}{40(1 - \frac{\nu_F}{10})} \right\}^2 + \frac{\nu_B\nu_F}{4},$$

where $s = \pm 1$, and the corresponding amplitudes, $\lambda_{AB}(s)$, are

$$\begin{aligned}\lambda_{AB}(+1) &\approx \begin{bmatrix} v_B u_{BA} \\ \left(3 + \frac{v_B}{2} + \frac{15v_2 - 12v_F - 4v_2v_F + v_F^2}{20 - 2v_F} + 2\sqrt{D_A}\right) u_{FA} \end{bmatrix}, \\ \lambda_{AB}(-1) &\approx \begin{bmatrix} \left(3 + \frac{v_B}{2} + \frac{15v_2 - 12v_F - 4v_2v_F + v_F^2}{20 - 2v_F} + 2\sqrt{D_A}\right) u_{BA} \\ -v_F u_{FA} \end{bmatrix}.\end{aligned}$$

The states with $s = 1$ and $s = -1$ are out-of-phase and in-phase, respectively, when $h < 0$ or $1 < h$, and they are opposite when $0 < h < 1$. In the boson-dominant approximation, in addition, the oscillation mode with $s = 1$ becomes similar with the FAB oscillation because of $X_B \ll X_F$ and $|v_B| \ll |v_F|$.

E. Collective Oscillation Modes in Largely Oblate Deformed Traps

Next we consider the mixtures in largely oblate deformed traps ($\omega_L \gg \omega_T$) when $\omega_f = 1$.

In this limit, solving (21), we have two bosonic and two fermionic intrinsic modes. Two bosonic oscillations are the boson longitudinal breathing (BLB) and the boson sideways breathing (BSB) modes:

$$\omega_{BLB}^2 \approx 3 \left(1 - \frac{v_B}{10}\right) \omega_L^2, \quad \omega_{BSB}^2 \approx \frac{10}{3} \left(1 - \frac{v_B}{10}\right) \omega_T^2.$$

The corresponding amplitudes are $\lambda_{BLB} \approx u_L \equiv {}^t(0, 1)$ and $\lambda_{BSB} \approx u_{BS} \equiv {}^t(1, 2/3)$. The BTB mode is a purely longitudinal oscillation, while the BSB mode includes the longitudinal and transverse oscillations with out-of-phases.

The fermion oscillation has also two modes: the fermion longitudinal breathing (FLB) and the boson sideways breathing (FSB) modes with the frequencies

$$\begin{aligned}\omega_{FLB}^2 &\approx \left(4 + \frac{v_2}{2} - \frac{3}{10}v_F\right) \omega_L^2, \\ \omega_{FSB}^2 &\approx 4 \left\{ 1 - \frac{v_F}{10} - \frac{(v_2 + \frac{v_F}{5})^2}{32 + 4v_2 - \frac{12v_F}{5}} \right\} \omega_T^2,\end{aligned}$$

and the amplitudes:

$$\lambda_{FLB} \approx u_L, \quad \lambda_{FSB} \approx u_{FS} \approx \begin{pmatrix} 1 \\ \frac{40v_2 + 8v_F}{40 + 5v_2 - 3v_F} \end{pmatrix}.$$

Now we show the collective oscillation in the case of largely oblate trap in full calculation, where longitudinal and the sideward-oscillation modes do not mix in the limit of $\omega_T/\omega_L \rightarrow 0$.

The longitudinal oscillation has two modes: the in-phase and out-of-phase longitudinal breathing (ILB

and OLB) modes, the frequencies of which are

$$\frac{\omega^2(s)}{\omega_L^2} = \frac{7}{2} - \frac{3v_B}{10} - \frac{3v_F}{10} + \frac{v_2}{2} + s\sqrt{D_L},$$

$$D_L = \left(1 + \frac{v_2}{2} - \frac{3v_F}{10} + \frac{3v_B}{10}\right)^2 + \frac{36}{100}v_Bv_F,$$

where $s = \pm 1$, and the corresponding amplitudes, $\lambda_{LB}(s)$, are

$$\lambda_{LB}(+1) \approx \begin{bmatrix} \frac{3}{5}v_B\mathbf{u}_L \\ \left(1 + \frac{3v_B}{10} + \frac{v_2}{2} - \frac{3v_F}{10} + \sqrt{D_L}\right)\mathbf{u}_L \end{bmatrix},$$

$$\lambda_{LB}(-1) \approx \begin{bmatrix} \left(1 + \frac{3v_B}{10} + \frac{v_2}{2} - \frac{3v_F}{10} + \sqrt{D_L}\right)\mathbf{u}_L \\ -\frac{3}{5}v_F\mathbf{u}_L \end{bmatrix}.$$

The sideways oscillation also has two modes: the in-phase and out-of-phase sideways breathing (ISB and OSB) modes, The frequencies are given by

$$\frac{\omega^2(s)}{\omega_F^2} = \frac{11}{3} - \frac{v_B}{6} - \frac{v_F}{5} - \frac{(v_2 + \frac{v_F}{5})^2}{16 + 2v_2 - \frac{6v_F}{5}} \pm \frac{s}{2}\sqrt{D_S},$$

$$D_S = \left\{ \frac{2}{3} + \frac{v_B}{3} + \frac{2v_F}{5} - \frac{(v_2 + \frac{v_F}{5})^2}{8 + v_2 - \frac{3v_F}{5}} \right\}^2 + \frac{9v_Bv_F}{25},$$

where $s = \pm 1$, and the corresponding eigenvectors, $\lambda_{SB}(s)$, are

$$\lambda_{SB}(+1) \propto \begin{bmatrix} \frac{9}{10}v_B\mathbf{u}_{BS} \\ \left\{ 1 + \frac{v_B}{2} - \frac{3v_F}{5} + \frac{3(v_2 + \frac{v_F}{5})^2}{16(1 + \frac{v_2}{8} - \frac{3v_F}{40})} + \frac{3}{2}\sqrt{D_S} \right\} \mathbf{u}_{FS} \end{bmatrix},$$

$$\lambda_{SB}(-1) \propto \begin{bmatrix} \left\{ 1 + \frac{v_B}{2} - \frac{3v_F}{5} + \frac{3(v_2 + \frac{v_F}{5})^2}{16(1 + \frac{v_2}{8} - \frac{3v_F}{40})} + \frac{3}{2}\sqrt{D_S} \right\} \mathbf{u}_{BS} \\ -\frac{9}{10}v_F\mathbf{u}_{FS} \end{bmatrix}.$$

In this limit the states with $s = 1$ and $s = -1$ are out-of-phase and in-phase, respectively, when $h < 0$ or $1 < h$, and they are opposite when $0 < h < 1$. In the boson-dominant approximation the oscillation mode with $s = 1$ becomes similar with the FAB oscillation

In all the limits, thus, the oscillation states are classified into two kinds of modes in the boson-dominant approximation. One is the boson and fermion co-moving, and the other is a fermion moving almost alone. When a large part of the condensed bosons occupy a single-particle state, the boson oscillation has the one-sided effect on the fermion oscillation. It is a characteristic properties of the collective oscillation of the BF mixture and has been seen also in the time-dependent approach [30, 33].

III. NUMERICAL RESULTS AND DISCUSSIONS FOR OSCILLATION MODES

In this section, we show the full calculation of the frequencies and amplitudes of the collective oscillation in the BF mixture obtained numerically. In actual calculations, we take the Yb-Yb system, where the numbers of the bosons and the fermions are $N_b = 30000$ and $N_f = 1000$, respectively. The parameters of the trapping potential are $\Omega_B = 2\pi \times (300^2 \times 50)^{\frac{1}{3}} \text{Hz}$ and $\omega_f = 1$; these values are almost similar with those in the experiments by Kyoto group [40] (the axial symmetry is a little broken in the actual experiment). The mass differences among Yb-isotopes can be safely neglected, so that we use the same mass and the same trap frequency ($\omega_f = 1$) for all Yb-isotopes in the calculation.

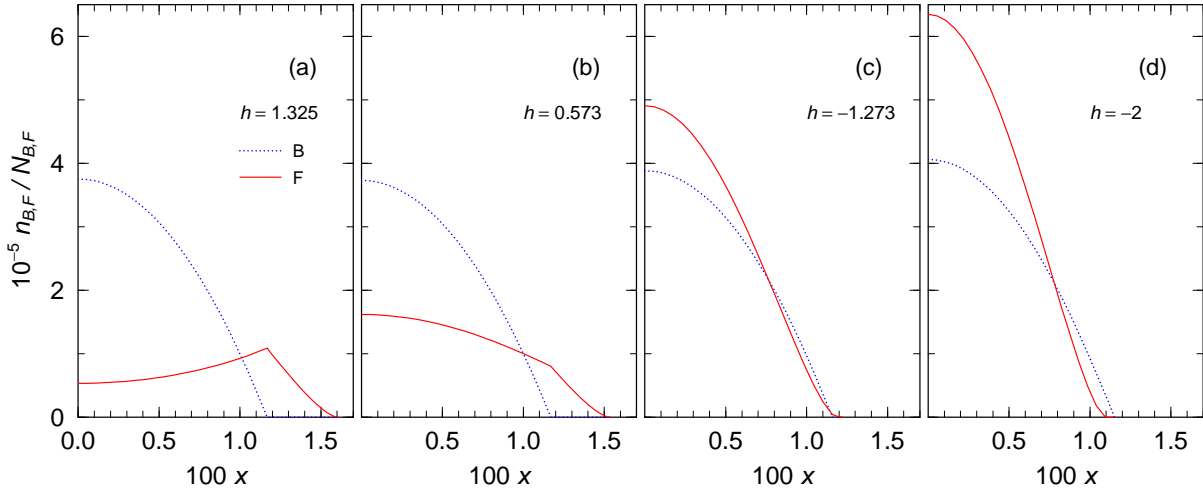


FIG. 1: (Color online) The ground-state density distributions of the BF mixtures in the TF approximation for $h = 1.325$ (a), 0.573 (b), -1.273 (c) and -2.5 (d). The dotted and solid lines are for the boson and fermion distributions. The numbers of the bosons and the fermions are $N_b = 30000$ and $N_f = 1000$, respectively. The parameters of the trapping potential are $\Omega_B = \Omega_F = 2\pi \times (300^2 \times 50)^{\frac{1}{3}} \text{Hz}$.

In Fig. 1, we show the scaled ground-state density distributions of boson (dotted line) and fermion (solid lines) for $h = 1.325$ (a), 0.573 (b), -1.273 (c) and -2.0 (d).

The boson densities are found to be center-peaked in all cases; in contrast, the fermion densities are surface-peaked in $h > 1$ (Fig. 1a), and center-peaked in $h < 1$. As the BF interactions becomes attractively stronger ($h < 0$), the fermions distribute more largely in the boson-distributed regions, and the boson density increases at the center [32–34].

For the boson number of $N_b = 30000$, the fermi gas is almost covered with the bose gas when $h < -1$. When $N_b = 10000$ [34], the bose gas partially distributes outside the boson region. The mixtures with large overlap region is expected to show significant behaviors of the collective oscillations more clearly, which is discuss later.

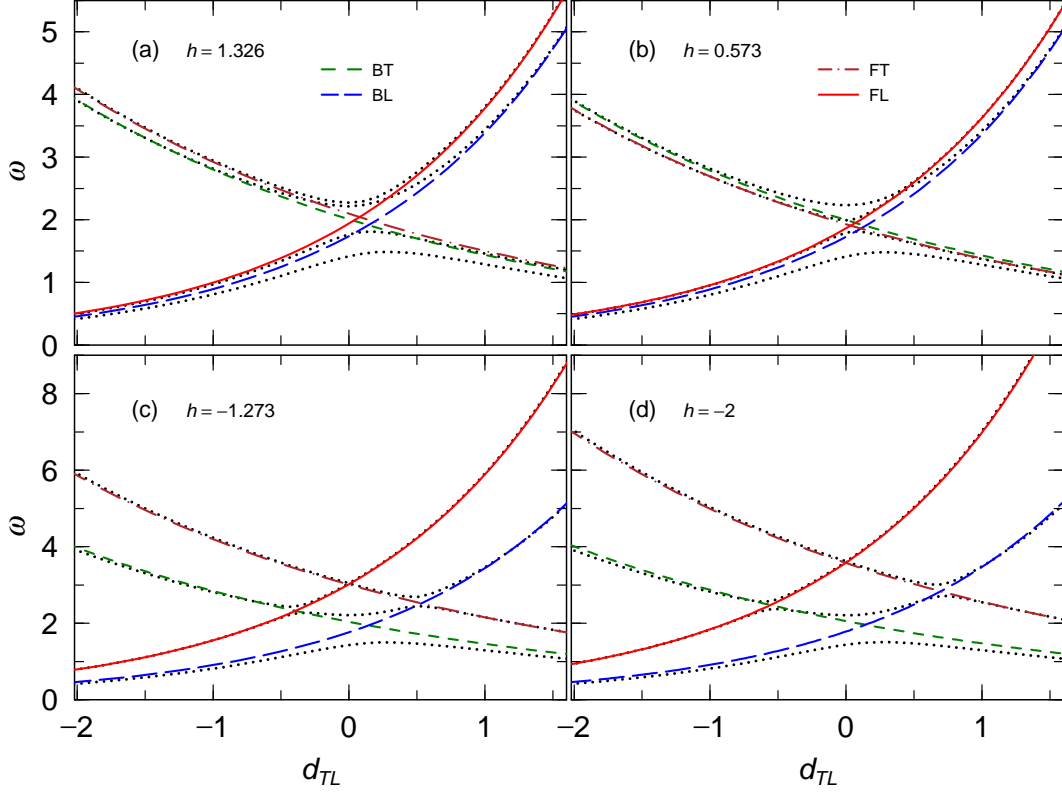


FIG. 2: (Color online) The frequencies of the collective oscillations versus the deformation parameters d_{TL} , which is defined in (24), when $h = 1.326$ (a) and $h = 0.573$ (b), $h = -1.273$ (c) and $h = -2$ (d). The dotted lines are for the frequencies in the full calculation in Eq.(18). The dashed, long-dashed, dot-dashed and solid lines denote the frequencies of the boson-transverse, boson-longitudinal, fermion-transverse and fermion longitudinal oscillations in (20).

In order to characterize the deformation of the system, we introduce the deformation parameter:

$$d_{TL} = \log \frac{\omega_L}{\omega_T}, \quad (24)$$

which is $d_{TL} > 0$ for prolate shapes, $d_{TL} = 0$ for spherical shapes, and $d_{TL} < 0$ for oblate shapes.

In Fig. 2, we show the d_{TL} -dependences of the frequencies of the breathing oscillations (dotted lines) solved in Eq. (18) for $h = 1.3255, 0.573, -1.273, -2$. We call the corresponding states as the state-1,2,3,4 in decreasing order of magnitudes. The intrinsic frequencies obtained in (20) are also plotted in Fig. 2, and, of course, they have crossing points. In Fig. 2, the level repulsion is not clear between the states-1 and -2 for $h < 0$ in the full calculations. However, the existence of the very small level gap is confirmed in more precise calculation, so that the frequencies represented with the dotted line in Fig. 2 show no crossings

We find that the intrinsic oscillation frequencies agrees with the full calculations except in the nearly-spherical region ($d_{TL} \approx 0$) and at the crossing points of the intrinsic frequencies, where the critical

changes of the collective frequency behaviors (dotted lines) occur: it is just level crossing phenomena.

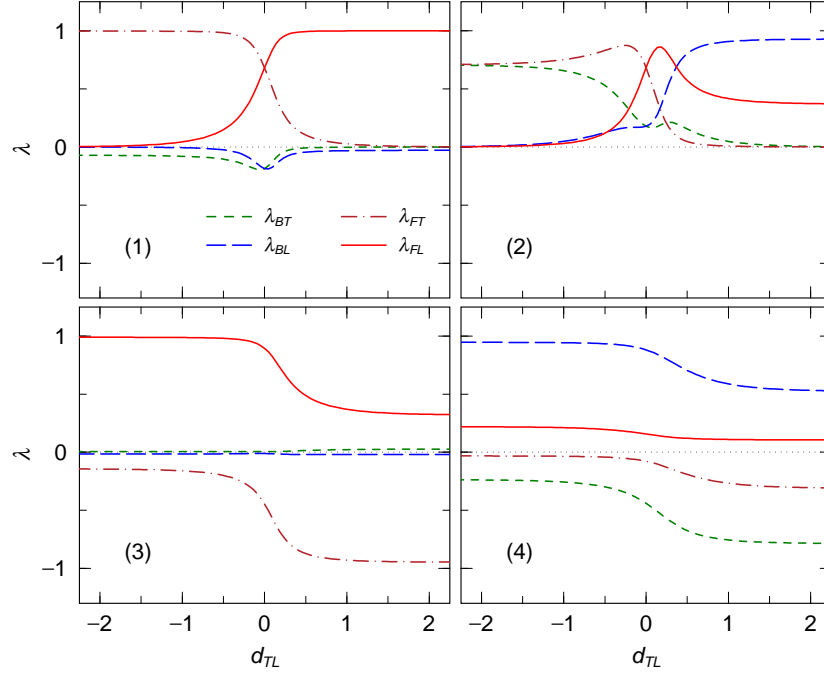


FIG. 3: (Color online) Components of the amplitudes for the state-1 (1), state-2 (2), state-3 (3) and state-4 (4) with $h = 1.326$. The dashed and long dashed lines represent the transverse and longitudinal components of the boson oscillations, respectively, and the dash-dotted and solid lines denote the transverse and longitudinal components of the fermion oscillations, respectively.

When $h = 1.326$ (Fig. 2a), the frequencies of the state-1 and -2 are very close for all deformation regions, and those of the state-3 and -4 are also close except the spherical region ($d_{TL} \approx 0$).

In order to understand the characteristics of these states, we show the strengths of the intrinsic-mode components included in the amplitudes for the state-1 \sim -4 (the panels 1 \sim 4) for $h = 1.326$ (Fig. 3), 0.573 (Fig. 4), -1.273 (Fig. 5), -2 (Fig. 6). The dashed and long-dashed lines represent the transverse (λ_{BT}) and longitudinal components (λ_{BL}) of the boson oscillations, respectively, and the dash-dotted and solid-lines denote the transverse (λ_{FT}) and longitudinal components (λ_{FL}) of the fermion oscillations, respectively.

From these figures, we can understand the character changes of the states in reference with the modes obtained in the previous sections.

As an example, we consider the character changes of the state-1 in $h = 1.326$. From the panel (1) of Fig. 3, we find that the λ_{FT} component is dominant in the largely prolate-deformed region ($d_{TL} \lesssim -1$), so that the state-1 is mainly in the FTB (OTB) mode. In the spherical region ($d_{TL} \approx 0$), we find the $\lambda_{FT} \approx \lambda_{FL}$; the state is in the FM (fermion monopole) mode. As explained in the previous section, it is really the OM (boson-fermion out-of-phase monopole) mode accompanying the small boson amplitudes;

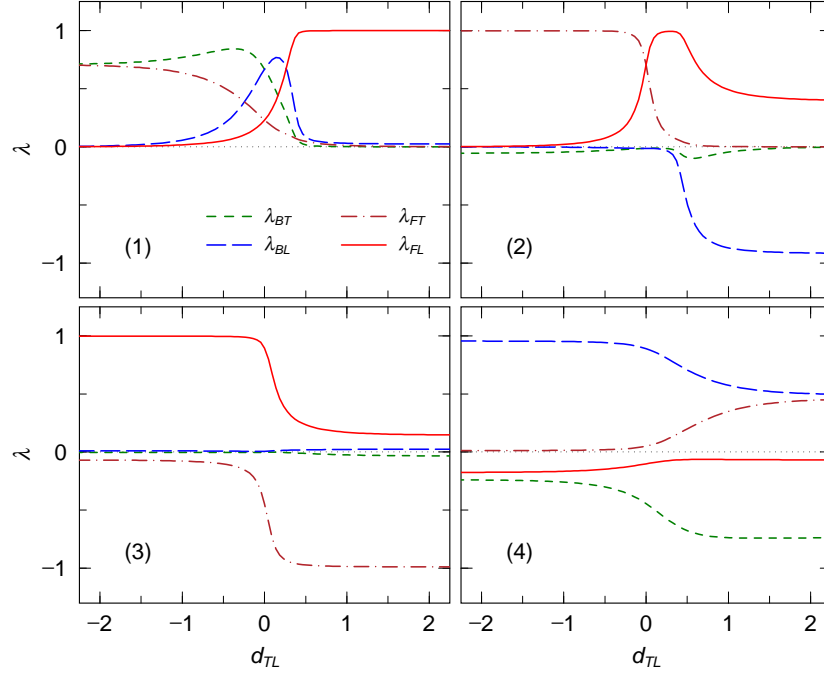


FIG. 4: (Color online) Components of the eigen-vectors of state-1 (1), state-2 (2), state-3 (4) and state-4 (4) with $h = 0.573$. The meanings of the lines are the same as those in Fig. 3.

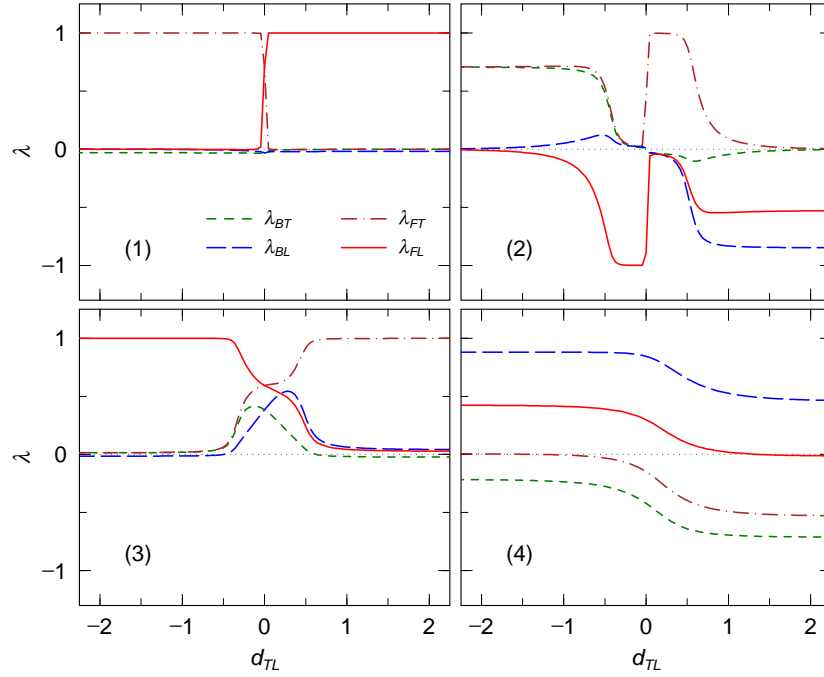


FIG. 5: (Color online) Components of the eigen-vectors of state-1 (1), state-2 (2), state-3 (3) and state-4 (4) with $h = -1.273$. The meanings of the lines are the same as those in Fig. 3.

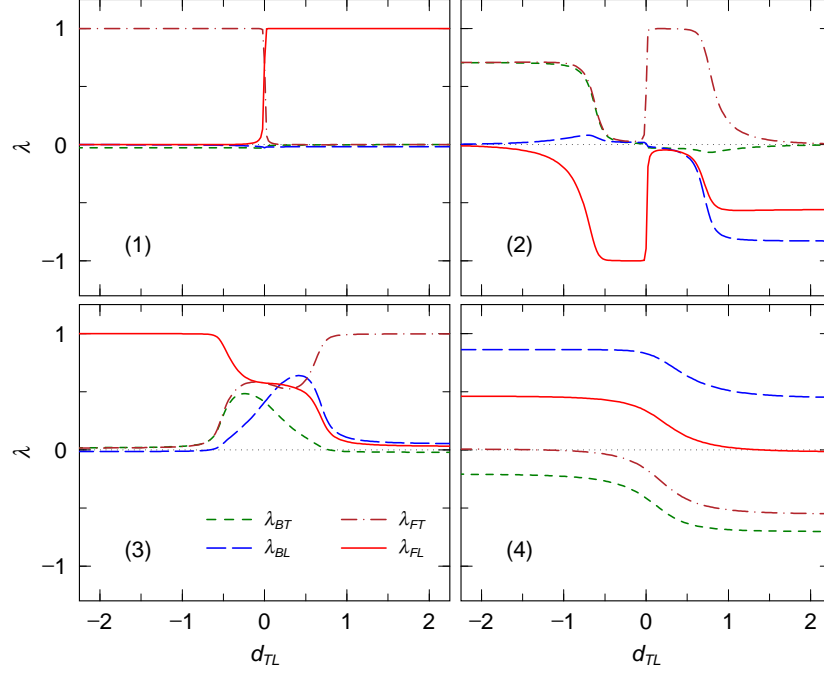


FIG. 6: (Color online) Components of the eigen-vectors of state-1 (a), state-2 (b), state-3 (c) and state-4 (d) with $h = -2$. The meanings of the lines are the same as those in Fig. 3.

we can find it in the small dips in the λ_{BT} and λ_{BL} lines in Fig. 3(1). We can find easily that the state-1 is in the FLB mode in the oblate region ($d_{TL} \gg 1$).

We analyze the character changes of the collective oscillations, in the same way, and show the results in Table. I.

h	state	prolate		spherical		oblate	
1.325	state-1	FTB (OTB)		OM		FLB (OLB)	
	state-2	ITB		IM		ILB	
	state-3	FAB (OAB)		FQ(OQ)		FSB (OSB)	
	state-4	IAB		IQ		ISB	
0.573	state-1	ITB		IM		FLB (ILB)	
	state-2	FTB (OTB)		FM (OM)		OLB	
	state-3	FAB (IAB)		FQ (IQ)		FSB (ISB)	
	state-4	OAB		OQ		OSB	
-1.273	state-1	FTB (OTB)		FM (OM)		FLB(OLB)	
	state-2	ITB	FAB	FQ (OQ)	FTB	ILB	
-2	state-3	FAB (OAB)		IM		FSB (OSB)	
	state-4	IAB		IQ		ISB	

TABLE I: Oscillation modes versus Deformation

The deformation regions of the system are classified into the prolate-deformed, semi-spherical and oblate-deformed ones. Furthermore, the oscillation behaviors and the order of their energy levels are also different in three regions of the BF interaction: $h > 1$, $1 > h > 0$ and $0 > h$.

As discussed in the previous section, the relative phase between the boson and fermion oscillations in the co-moving oscillation modes when $0 < h < 1$ show different behavior from that in other cases except the ITB and OTB modes in the largely prolate deformation.

When the BF interaction is repulsive, $h > 0$, the mode changes are simple, and the in-phase and out-of-phase modes do not appear in the states.

When the BF interaction is attractive, $h < 0$, the mode changes become complicated, especially in the semi-spherical deformation region. When the deformation of the system becomes large (in either prolate or oblate shapes), the oscillation behaviors are simple; the four states becomes the intrinsic modes which are defined in the previous section.

As the deformation approaches to the spherical one, the oscillation modes show drastic changes between the fermion-dominant and the Bf co-moving modes, and between the in-phase and out-of-phase modes. The mixing of the oscillation modes varies complicatedly in the transcendental regions around the spherical shape.

In addition, we should note that, in the completely spherical system, the oscillations are decoupled into the monopole and quadrupole modes, but this decoupled behavior appears only in the very narrow region around $d_{TL} \approx 0$.

Thus, the oscillation modes in each state have the characters varying with the deformation of the trap. We should comment that more drastic mode changes appear for the variation of the BF-coupling h is varied [30, 33, 34]

The ranges of the transcendental regions are approximately estimated as the region between the two crossing points at the deformation points d_1 and d_2 in Fig. 2; the crossing of BLB and FTB corresponds to d_1 , and that of BTB and FLB corresponds to d_2 .

The points d_1 and d_2 are calculated from the crossing conditions $\omega_{BT} = \omega_{FL}$ and $\omega_{BL} = \omega_{FT}$, respectively. Using Eqs. (20), we obtain

$$d_1 = \frac{1}{2} \log \left[\frac{4 \left(1 - \frac{v_E}{10}\right)}{3 \left(1 - \frac{v_B}{10}\right)} \right], \quad (25)$$

$$d_2 = \frac{1}{2} \log \left[\frac{4 \left(1 - \frac{v_E}{10}\right)}{\left(4 - \frac{3v_E}{10} + \frac{v_2}{2}\right)} \right]. \quad (26)$$

In Fig. 7, we show the level-crossing points d_1 and d_2 (a and b) when $N_b = 4000$ (dotted line), $N_b = 10000$ (dashed line), $N_b = 30000$ (solid line) and $N_b = 50000$ (dot-dashed line), respectively. When $N_b \gtrsim 30000$, the d_1 and d_2 are found to be almost independent of N_b . In addition, the order of d_1 and d_2 are

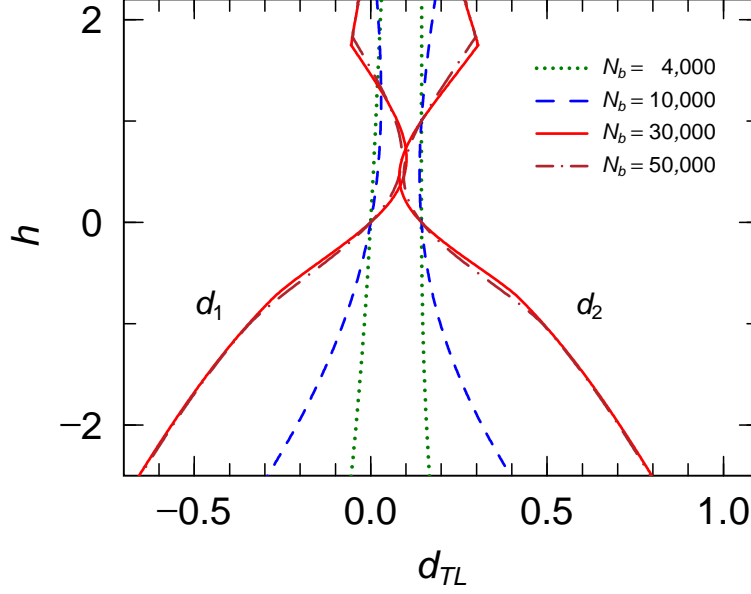


FIG. 7: (Color online) The level-crossing point of the deformation parameter between the BLB and FTB modes, d_1 , (a) and that between the BTB and FLB modes, d_2 (b), when $N_f = 1000$. The dotted and dashed, solid and dotted-dashed lines represent the results when $N_b = 4000, 10,000, 30,000$ and $50,000$, respectively.

exchanged in $0.37 \lesssim h \lesssim 0.73$ when $N_b \lesssim 30000$.

Let's give the qualitative explanations of the N_b -independence of the critical points in the boson-dominate approximation ($N_b \gg N_f$). When $N_b \gg N_f$, the boson density distribution becomes robust and is not affected so much by the fermion density, so that it becomes $n_B(x) \approx e_B - x^2$. In the case of $h < 0$, the fermions populate inside the boson region, and the TF equation (9) gives the fermion density distribution:

$$n_F \approx \{ (e_F - h e_B) - (1 - h)x^2 \}^{\frac{3}{2}},$$

which is determined by $e_F - h e_B$, whose value is also decided by the fermion number. In $0 < h \ll 1$ (the very weak BF interaction), the large part of fermions populate in the boson region, and the argument for $h < 0$ is also available.

Next, when $h \approx 1$, $\partial n_F / \partial x \approx 0$ and $\partial n_B / \partial x \approx -2x$ inside the boson region, so that, using (16), we obtain $V_1 \approx 0$, which leads to $v_B = V_1 / X_B \approx 0$ and $v_F = V_1 / X_F \approx 0$. Substituting these values into (25) and (26), we obtain $d_2 \approx \log(4/3)/2 \approx 0.14$. Because inside the boson region in addition, $V_2 \rightarrow 0$ when $N_f / N_b \rightarrow \infty$, and $V_2 \rightarrow -2hX_F$ when $N_f / N_b \rightarrow 0$, namely $v_2 \approx 0$ when $N_b \ll N_f$ and $v_2 \approx -2$ when $N_b \gg N_f$. Thus, we obtain $d_1 \approx 0$ when $N_b \ll N_f$, and $d_2 \approx \log(4/3)/2 \approx d_1$ when $N_b \gg N_f$.

Finally, in $h > 1$, the fermion density distribution has the surface-peaked peak, and a large part of fermions populate outside the boson region. The oscillation behavior is also determined by the density distribution around the boson surface, which does not so strongly depend on the boson numbers. Thus, the level-crossing points are almost independent of N_b when $N_b \gg N_f$.

We should note that if $N_b \approx N_f$ or $N_b \ll N_f$, the fermions distribute largely outside of the boson region, and the overlap region of the bosons and fermions is very small. Then, the bose gas and fermi gas oscillate almost independently [26] and their oscillation behaviors are not so interesting.

The critical phenomena originated in the level crossing phenomena are seen only for the large values of $d_{1,2}$. Hence we should focus this study on the system with $N_b \gtrsim 30N_f$ and $h < -1$, where the fermions distribute inside the boson region.

In this system, the boson motions are rarely affected by the fermions, lead to the forced oscillations of fermions, which are the boson-fermion co-moving oscillations. On the other hand, the fermion oscillation does not largely affect the boson oscillation, and then there are other kinds of the intrinsic modes where the fermions oscillate dominantly with very weakly oscillations of bosons. In this oscillation, the fermion potential is equivalent to the harmonic-oscillator potential with the shape of $he_B + (1-h)x^2$.

When the deformation parameters is in the regions of $d_1 < d_{TL}$ and $d_{TL} < d_2$, the oscillation behavior becomes the same as that in the extremely deformed limit. For $d_{TL} < d_{TL} < d_1$, the mixings of the oscillation modes occur and cause the variations of their characters. Especially, in the state-2 and the state-3, the oscillation behavior changes critically around $d_{TL} \approx d_1$ and $d_{TL} \approx d_2$.

IV. COMPARISONS WITH THE DYNAMICAL APPROACH

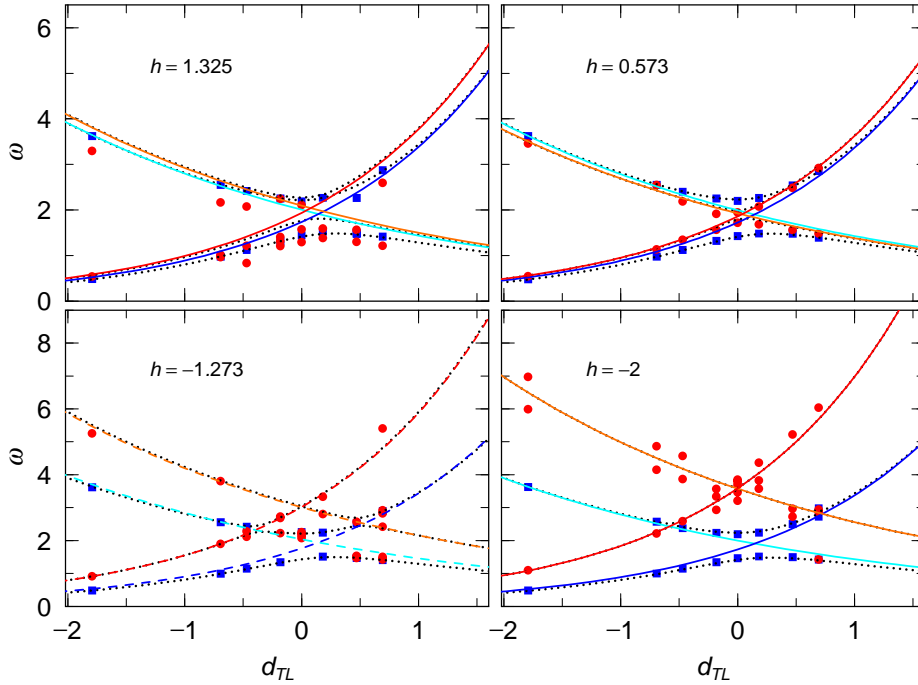


FIG. 8: (Color online) The frequencies of the collective oscillations in the BF mixtures obtained by the TDGP+Vlasov approach (solid squares and open circles). The lines are the collective and the intrinsic frequencies obtained in the scaling method, which are the same ones in Fig. 2.

In Fig. 8, we show the frequencies of the collective oscillation in the BF mixture calculated in the dynamical approach based on the TDGP+Vlasov equation; the derivations and the details of this method was given in our previous paper[30, 32–34]. We find that these two methods give the consistent results except in the case of the strong boson-fermion attractive interactions.

We should comment that the dynamical calculations give consistent results with the RPA and its approximation like the scaling method in early stage of time development. But it show discrepancies in later stage, and, as the boson-fermion interaction becomes stronger, the discrepancies appear earlier in the time-development. Thus, the BF mixtures show new dynamical properties different from the other kinds of finite many-body system such as atomic nuclei.

V. SUMMARY

In this paper, we have investigated the deformation dependence of the breathing oscillations in the boson-fermion mixture. The deformation regions are classified into the prolate, semi-spherical and oblate ones. In each region, the four kinds of oscillations with different mixing characters, the BLB, BTB, FLB and FTB modes, appear; around the borders of these regions, the level-crossing phenomena between the BTB and FLB and between the BTB and FLB modes occurs.

This classification based on the deformation of the system should be useful for experimentalists in the observation of these breathing oscillations and/or related phenomena. Furthermore, the oscillation behaviors become complicated in the region between the largely deformed and spherical shapes, and the drastic changes occur at the level crossing points; the resonant oscillations should appear at the level crossing points.

These variations of the oscillational behaviors are clearly seen in the case of the strong boson-fermion attractive interaction ($h \lesssim -1$), and the mixtures of the large boson number ($N_b \gg N_f$), where the boson-dominant approximation is available.

When $N_b \gg N_f$, the oscillation states are mainly classified into two kinds: boson-fermion co-moving modes and fermion-dominant oscillation modes. The co-moving oscillation modes are actually the boson dominant oscillation with the forced-oscillation of fermions; the frequencies of the boson and fermion oscillations are the same.

In the time-dependent simulations [32–34], the fermionic intrinsic oscillations show rapid damping, and, particularly when $h \gtrsim 1$, their amplitudes are negligibly small. The strength of the fermion intrinsic oscillation is separated into the two oscillation modes corresponding to fermion motions inside and outside of the boson populate region; [32–34]: these behaviors cannot be described with the scaling method. When the BF-interaction is repulsive, large part of fermions populate outside of the boson

region, and, when $h > 1$, the fermions outside the boson region dominate. Thus, the fermion dominant oscillation do not exist in long period, and we cannot easily observe these modes in actual experiments. On the other hand, the boson-fermion co-moving oscillations can be easily observed in experiments. Indeed, the BLB oscillations have been found in the actual experiments [39], which showed the 1.2% increase of its frequency when the BF coupling is varied from $h_{BF}/g_{BB} = 0$ to $h_{BF}/g_{BB} = 1.325$. In this experiment, because of the strongly-repulsive BF interaction, the fermion contribution should be small. In the case of the strongly-attractive BF interaction ($h < -1$), however, we can observe larger effects of the deformation in the oscillation behaviors, and find that the clear differences between the spherical and non-spherical oscillations. The BF mixtures of the strongly-attractive BF interactions also show the oscillation behaviors caused by the fermion-gas expansion [31, 33, 34]. This behavior cannot be included in the scaling method.

In order to obtain precise results of the oscillation behaviors of the BF mixtures, especially around the level-crossing points, the analysis based on the calculations of the time-dependent framework with the TDGP+Vlasov approach. The details of the deformation dependence of the time-development behaviors of the BF mixtures should be given in the other paper.

Acknowledgment

This work is supported in part by the Japanese Grand-in-Aid for Scientific Research Fund of the Ministry of Education, Science, Sports and Culture (21540212 and 22540414) and Nihon University College of Bioresource Sciences Research Grant for 2013.

-
- [1] E.A. Cornell and C.E. Wieman, Rev. Mod. Phys. **74**, 875 (2002);
W. Ketterle, Rev. Mod. Phys. **74**, 1131 (2002).
 - [2] F. Dalfovo, et al., Rev. Mod. Phys. **71**, 463 (1999).
 - [3] C.J. Pethick and H. Smith, "Bose-Einstein Condensation in Dilute Gases", Cambridge University Press (2002).
 - [4] J.O. Andersen, Rev. Mod. Phys. **76**, 599 (2004).
 - [5] A.G. Truscott, K.E. Streker, W.I. McAlexander, G.B. Partridge and R.G. Hulet, Science **291**, 2570 (2001).
 - [6] G. Rotor, F. Riboli, G. Modugno and M. Inguscio, Phys. Rev. Lett. **89**, 150403 (2002).
 - [7] B. DeMarco and D.S. Jin, Science **285**, 1703 (1999);
S.R. Granade, M.E. Gehm, K.M. O'Hara, J.E. Thomas, Phys. Rev. Lett. **88**, 120405 (2002).
 - [8] F. Schreck, et al., Phys. Rev. Lett. **87**, 080403 (2001).
 - [9] Z. Hadzibabic, et al., Phys. Rev. Lett. **88**, 160401 (2002); *ibid* **91**, 160401 (2003).
 - [10] M. Modugno, F. Ferlaino, F. Riboli, G. Roati, G. Modugno, M. Inguscio, Science **297**, 2240 (2002);
Phys. Rev. A **68**, 043626 (2003).

- [11] H. Feshbach, Ann. Phys. (NY) **19**, 287 (1962).
- [12] K. Mølmer, Phys. Rev. Lett. **80**, 1804 (1998).
- [13] M. Amoruso, A. Minguzzi, S. Stringari, M. P. Tosi and L. Vichi, Eur. Phys. J. D **4**, 261 (1998).
- [14] M.J. Bijlsma, B.A. Heringa and H.T.C. Stoof, Phys. Rev. A **61**, 053601 (2000).
- [15] L. Vichi, M. Inguscio, S. Stringari, and G.M. Tino, Eur. Phys. J. D **11**, 335 (2000).
- [16] L. Vichi, M. Inguscio, S. Stringari and G.M. Tino, J. Phys. B: At. Mol. Opt. Phys. **31** L899 (1998).
- [17] T. Miyakawa, K. Oda, T. Suzuki and H. Yabu, J. Phys. Soc. Japan **69**, 2779 (2000).
- [18] N. Nygaard and K. Mølmer, Phys. Rev. A **59**, 2974 (1999).
- [19] X.X. Yi and C.P. Sun, Phys. Rev. A **64**, 043608 (2001).
- [20] L. Viverit, C.J. Pethick and H. Smith, Phys. Rev. A **61**, 053605 (2000).
- [21] P. Capuzzi and E.S. Hernández, Phys. Rev. A **66**, 035602 (2002).
- [22] P. Capuzzi, A. Minguzzi and M.P. Tosi, Phys. Rev. A **68**, 033605 (2003).
- [23] T. Miyakawa, T. Suzuki and H. Yabu, Phys. Rev. A **64**, 033611 (2001).
- [24] R. Roth and H. Feldmeier, Phys. Rev. A **65**, 021603(R) (2002).
- [25] P. Capuzzi and E. S. Hernández, Phys. Rev. A **64**, 043607 (2001).
- [26] T. Sogo, T. Miyakawa, T. Suzuki and H. Yabu, Phys. Rev. **A66**, 013618 (2002);
T. Sogo, T. Suzuki and H. Yabu, Phys. Rev. **A68**, 063607 (2003).
- [27] T. Miyakawa, T. Suzuki and H. Yabu, Phys. Rev. A **62**, 063613 (2000).
- [28] A. Minguzzi and M.P. Tosi, Phys. Lett. A **268**, 142 (2000).
- [29] S.K. Yip, Phys. Rev. **A64**, 023609 (2001).
- [30] T. Maruyama, H. Yabu and T. Suzuki, Phys. Rev. **A72**, 013609 (2005).
- [31] T. Maruyama, H. Yabu and T. Suzuki, Lazer Physics, **15**, 656 (2005).
- [32] T. Maruyama and G.F. Bertsch, Phys. Rev. **A77**, 063611 (2008)
- [33] T. Maruyama and H. Yabu, Phys. Rev. **A80**, 043615 (2009).
- [34] T. Maruyama and H. Yabu, J. Phys. **A80**, 043615 (2009).
- [35] Y. Takasu, et al., Phys. Rev. Lett. **91**, 040404 (2003).
- [36] T. Fukuhara, S. Sugawa, and Y. Takahashi, Phys. Rev. **A76**, 051604(R) (2007).
- [37] T. Fukuhara, Y. Takasu, M. Kumakura and Y. Takahashi, Phys. Rev. Lett. **98**, 030401 (2007).
- [38] K. Enomoto, M. Kitagawa, K. Kasa, S. Tojo and Y. Takahashi, Phys. Rev. Lett. **98**, 203201 (2007); M. Kitagawa, et.al., Phys. Rev. **A77**, 012719 (2008).
- [39] T. Fukuhara, et al., Appl.Phys. **B96**, 271 (2009).
- [40] T. Fukuhara, master thesis, Kyoto University, Kyoto (2009).
- [41] T. Maruyama and T. Nishimura, Phys. Rev. **A75**, 033611 (2007).
- [42] T. Maruyama and G.F. Bertsch, Phys. Rev. **A73**, 013610 (2006).
- [43] G.F. Bertsch, Nucl. Phys. **A249**, 253 (1975);
D.M. Brink and Leobardi, Nucl. Phys. **A258**, 285 (1976).
- [44] G.F. Bertsch and K. Stricker, Phys. Rev. **C13**, 1312 (1976);
T. Suzuki, Prog. Theor. Phys. **64**, 1627 (1980).

- [45] O. Bohigas, A.M. Lane and J. Martorell, Phys. Rep. **51**, 267 (1979),
- [46] Y. Castin and R. Dun, Phys. Rev. Lett. **77**, 5315 (1996).
- [47] M.-O. Mewes, et al., Phys. Rev. Lett. **77**, 988 (1996).
- [48] Y. Kagan, E.L. Surkov and G.V. Shlyapnikov, Phys. Rev. **A54**, R1753 (1996).
- [49] T. Nishimura and T. Maruyama, J. Phys. Soc. Jpn. **81**, 044001 (2012).